Nuclear Instruments and Methods in Physics Research A 652 (2011) 201–204

Contents lists available at ScienceDirect

Nuclear Instruments and Methods in Physics Research A

journal homepage: www.elsevier.com/locate/nima

# $LaCl_3$:Ce coincidence signatures to calibrate gamma-ray detectors

Justin I. McIntyre*, Brian T. Schrom, Mathew W. Cooper, Anthony Day, James C. Hayes, Tom R. Heimbigner, Charles W. Hubbard, Michael D. Ripplinger, Reynold Suarez

*Pacific Northwest National Laboratory, 902 Battelle Boulevard P.O. Box 999, Richland Washington, WA 99353, USA*

ARTICLE INFO

Available online 24 February 2011

*Keywords:*
Lanthanum-Tri-Chloride
Radiation detector
Calibration
Coincidence techniques

ABSTRACT

Calibrating the gamma-ray detection efficiency of radiation detectors in a field environment is difficult under most circumstances. To counter this problem we have developed a technique that uses a Cerium doped Lanthanum-Tri-Chloride ($LaCl_3$:Ce) scintillation detector to provide gated gammas (Guillot-Noël et al. (1999) [1] and van Loef et al. (2001) [2]). Exploiting the inherent radioactivity of the $LaCl_3$:Ce due to the long-lived radioactive isotope $^{138}$La ($t_{1/2}=1.06\times10^{11}$ yr) allows the use of the 788 and 1436 keV gammas as a measure of efficiency. In this paper, we explore the effectiveness of using the beta-gamma coincidences radiation $LaCl_3$:Ce detector to calibrate the energy and efficiency of a number of gamma-ray detectors.



## 1. Introduction

Field environments for radiation detectors have proven to be difficult locations for most detailed calibration regimes. Along with the difficulty of maintaining and reproducing precise geometries, increasing regulatory constraints are making it difficult to carry calibration radiation sources into the field environment. Good energy calibration can usually be achieved for lightly shielded detectors via the naturally occurring background isotopes of $^{40}$K, $^{238}$U, and $^{232}$Th and their respective daughter products. However, the changing environmental background levels mean that these same naturally occurring isotopes cannot be used for efficiency calibrations and they may have large variations in concentrations (radon and radon daughter products are good examples). To counter these problems an application using a Lanthanum-Tri-Chloride detector doped with Cerium ($LaCl_3$:Ce) has been investigated at PNNL as an effective infield source to provide both absolute detection efficiency and energy calibrations.

Lanthanum-Tri-Chloride and its twin $LaBr_3$:Ce: have been seen as the new standard in large volume, room temperature, gamma-ray detector with superior resolution (~3%@662 keV) [3,4]. The first commercial crystals suffered from high alpha contamination that was determined to be Ac-227 contamination [5,6]. Subsequent crystal production methods managed to decrease this contamination to acceptable levels, but still left the dominant radioactive isotope $^{138}$La ($t_{1/2}=1.05\times10^{11}$ yr). The effectiveness of using the beta-gamma coincidences properties of a $LaCl_3$:Ce detector to calibrate the energy and efficiency of HPGe and NaI:Tl detectors has shown some promising results.

## 2. Experimental

The decay scheme for $^{138}$La is located in Fig. 1, which shows two decay mechanisms [7]. The most energetic decay is via electron capture (EC) followed by a 1435.8 keV gamma ray and subsequent emission of a 31.8–37.5 keV Barium X-ray [8,9].[1] The second emission is via beta decay (255 keV endpoint energy) and a 788.7 keV gamma-ray. Both of these decays provide good coincidence detection particles, the X-rays and beta particles for the small $LaCl_3$:Ce detector and the two gamma rays for the test detector under consideration. The low energy of the $^{138}$La X-rays meant that they are efficiently detected in the $LaCl_3$:Ce crystal, and the beta particles are detected because they are charged particles. In addition, the small size of the crystal causes a low detection probability of the two gamma rays in the $LaCl_3$:Ce crystal, but can be detected in the larger HPGe and NaI:Tl detectors under consideration.

### 2.1. Test detectors

The $LaCl_3$:Ce crystal used in this study was the largest commercially available detector at the time of purchase in 2004 and was 38 mm long by 38 mm in diameter [3]. The NaI:Tl detector was a standard 50 mm thick by 127 mm diameter unit,

* Corresponding author. Tel.: +1 509 376 0085; fax: +1 509 372 0672.
*E-mail address:* justin.mcintyre@pnl.gov (J.I. McIntyre).

0168-9002/$ - see front matter © 2011 Elsevier B.V. All rights reserved.
doi:10.1016/j.nima.2011.02.072

[1] Substantial differences exist between the printed version of the x-ray intensities in the Table of Radioactive Isotopes and the online version. The online version appears to be more recent and was used.

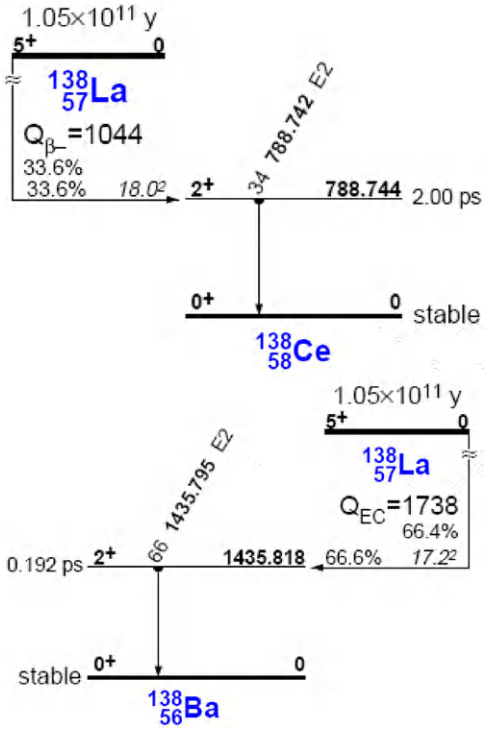


**Fig. 1.** $^{138}$La decay schemes from Ref. [7].

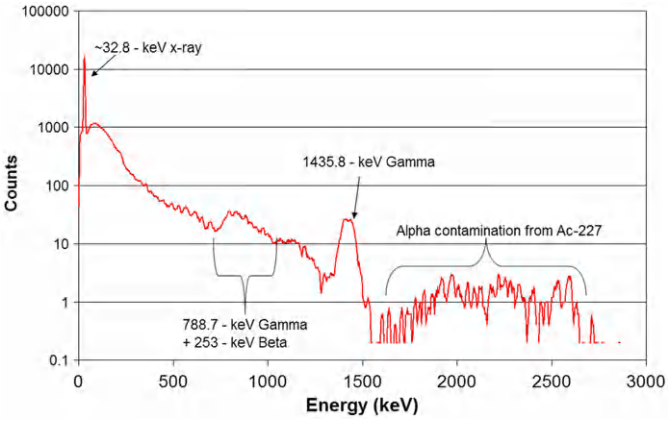


**Fig. 2.** Lanthanum tri-chloride spectrum showing the various gamma rays, X-rays, and charged particles (count time was 10,000 s). Note the presence of the $^{227}$Ac alphas.

**Table 1**
Energy and branching ratios for $^{138}$La [7].

| Energy (keV) | Branching ratio (%) |
|---|---|
| 31.8 | 26.3 |
| 32.2 | 14.30 |
| 36.4 | 7.27 |
| 37.5 | 1.84 |
| 788.7 | 32.9 |
| 1435.8 | 67.1 |

which has been characterized by the SYNTH program [10,11]. The HPGe detector had the efficiency of 140% of a standard 76 mm × 76 mm NaI:Tl detector [12]. The detector readout electronics was done using XIA's 4 channel PIXIE-4™ analog to digital cards and the high voltage supply was a PNNL built 4-channel PXI card [13]. In addition, the detectors used a Canberra 2005 fast pre-amplifier to provide pulse-shaping from the photo-multiplier tubes.

### 2.2. Radioactive decays

The rate of $^{138}$La decays in the $LaCl_3$:Ce was calculated to be 75.8 ± 1.8 Bq. It was derived from the known concentration of $^{138}$La (0.0902% of naturally occurring La) and the total amount of lanthanum in the detector, assuming the dimensions provided by Saint Gobain. An experimental verification of this rate was done using the ~32.8 keV X-rays as seen in a spectrum taken of the $LaCl_3$:Ce in a 5 cm lead cave (Fig. 2). The spectrum clearly shows the intrinsic radiation features of the $^{138}$La along with some low level alpha contamination from $^{227}$Ac contamination [6]. The energies and branching ratios for the X-rays and gamma rays are shown in Table 1 and were used to determine an activity of 56.2 ± 1.2 Bq for the $^{138}$La, which was within 75% of the expected result from volumetric considerations. Not taken into consideration was the geometric effect for radiation that did not intersect the detector (the outer ~2 mm of material). The coincidence gamma ray (1435.8 keV) was detected ~1.5% of the time, indicating the poor stopping power of the $LaCl_3$:Ce crystal for high energy gammas.

### 2.3. Two-dimensional histograms

By plotting the energy response in the $LaCl_3$:Ce detector against the energy response in each of the test detectors it was possible to define regions of interest to accurately account for the total counts in the 789 and 1436 keV energy peaks. Fig. 3 shows the 2-dimensional histogram of the response from the $LaCl_3$:Ce detector versus the response of the HPGe detector. Several key features are present in the histogram. The 788 keV gamma shows up in coincidence with the beta near the midpoint of the *y*-axis. The 32.8 keV X-ray and 1436 keV gamma coincidence can be seen close to the *y*-axis on the top (see the inset for more detail). In addition the Compton scatter line from the 1436 keV gamma is evident as the diagonal strip which represents constant energy of 1436 keV is shared between the two detectors.

This coincidence feature can be used to provide a good energy calibration for the HPGe detector, if the $LaCl_3$:Ce detector is energy calibrated (Reeder et al. [14] provide a detailed description of this process for a beta-gamma detector). In addition to energy sharing between the detectors, there is also the process of a detection of the X-rays in the $LaCl_3$:Ce and a partially detected 1435.8 keV gamma in the HPGe. This process appears as the red vertical line at ~32.8 keV on the $LaCl_3$:Ce axis. The same processes can occur for the 788.7 keV gamma but the beta energy distribution causes the process to show up as a wide diagonal band for dual $LaCl_3$:Ce–HPGe Compton scattering and a wide vertical band from 0–788.7 keV along the vertical axis for HPGe only Compton scattering.

## 3. Results

### 3.1. Pulse shape discrimination

A second approach to determine the absolute source strength of the detector would be to use the 788.7 keV gamma and the coincident beta. To try to get at a clean beta spectrum, pulse-shape-discrimination (PSD) techniques were applied to the data. A previous paper by Hoel et al. [15] has shown that it is possible

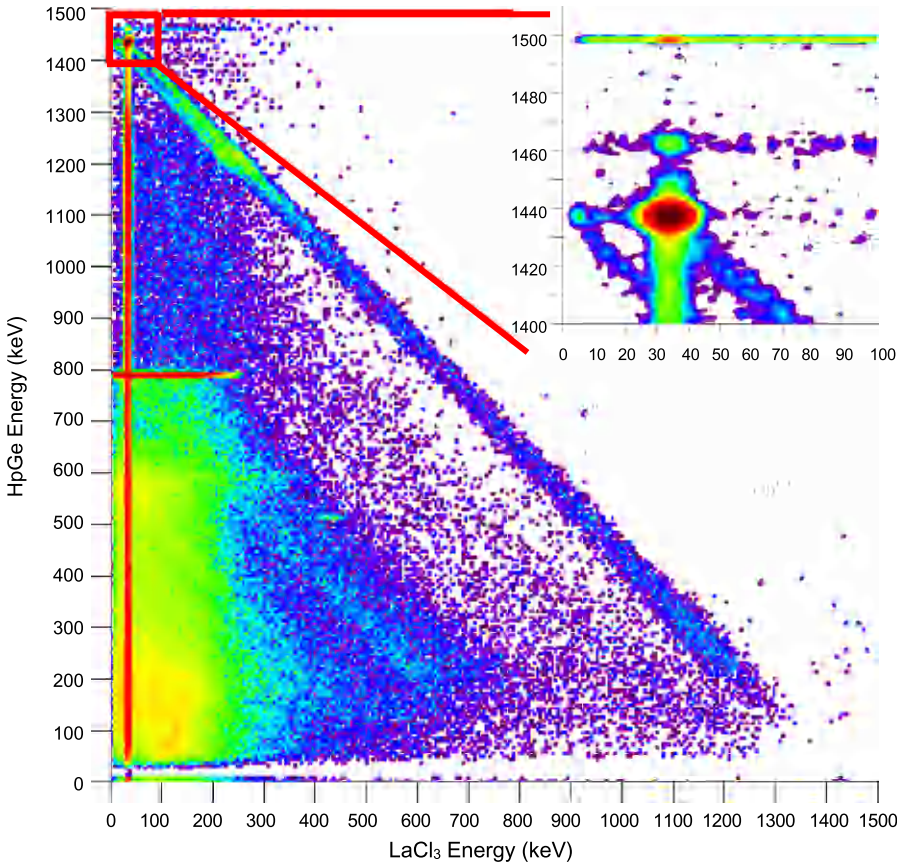


**Fig. 3.** Two-dimensional plot of the LaCl3:Ce detector response versus the HPGe detector response. The inset is a blowup of the HPGE 1468 keV region.

to discriminate between alpha particles and gamma rays in scintillators. The internal X-rays and beta particles offered an ideal environment to test PSD between photons and charged particles. By making tight cuts around the beta distribution at 788 and 32.8/1436 keV coincidence feature it is possible to choose an almost pure beta signature or pure X-ray (photon) signature within the $LaCl_3$:Ce detector. Fig. 4A shows the HPGe coincidence spectrum with the two prominent gamma rays from the $LaCl_3$:Ce. Fig. 4B shows the spectrum that results for the $LaCl_3$:Ce when only the data that falls between the dashed lines is plotted. The beta spectrum has very little interference from the ~32.8 keV X-rays and the X-rays have very little Compton continuum or beta signals. By plotting an average of the digitized pulses from each of these regions it is possible to determine if there are differences between the two processes. This test showed that there is no easy method to separate out the two decay processes on a pulse by pulse basis. Future work may follow this same technique but with faster digitization electronics (~1 ns) to probe smaller rise-time or decay-time differences.

### 3.2. NaI:Tl detector efficiency

The spectrum obtained for the NaI:Tl detector had several important features that demonstrate the utility of having a gated gamma-ray source in a field environment. Fig. 5 shows three histograms. The lower of three is the coincidence spectrum (gating the NaI:Tl with the LaCl3:Ce). The detector energy scale is easily determined with the two available peaks, which are clearly delineated. The detector efficiency is either checked against the earlier laboratory/depot level calibration (highest level of accuracy) or determined in the field via the counts in the two peaks, corrected for detector dead-time and branching ratio for each gamma ray. The lower of the two upper curves is the background of the NaI:Tl detector during the same testing period and the upper curve is the sum of the $LaCl_3$:Ce coincidence curve and the background curve (i.e. the total spectrum collected by the NaI:Tl detector during the testing period). What becomes apparent is the enhanced signal to noise ratio of the coincidence spectrum (lower curve) over the total spectrum (top curve) even in the presence of a significant background source term (middle curve). There was no attempt made to shield the NaI:Tl detector to fully illustrate the power of the gated gamma-ray source ($LaCl_3$:Ce).

The high resolution of the HPGe detector showed both 1435.8 and 1461 keV peaks clearly but detectors with lower resolution (NaI:Tl CsI:Tl, etc.) do not allow such separations. The total benefits from the enhanced signal to noise ratio allow the use of a relatively weak source, ~2 nCi, with no additional shielding.

### 3.3. Plastic scintillation energy calibration

The use of plastic scintillation paddles in radiation detection applications provides a robust and less expensive option than modest spectroscopic solutions (NaI:Tl, CsI:Tl, etc.). The drawbacks to using plastic are the low resolution for charged particles (25–10% depending on energy) and the very low resolution that is obtained from gamma-ray sources. Some attempts have been made to use the distribution of Compton scattering events in plastic to characterize gamma-ray sources. In order to do this, basis spectra must be taken in the laboratory for comparison

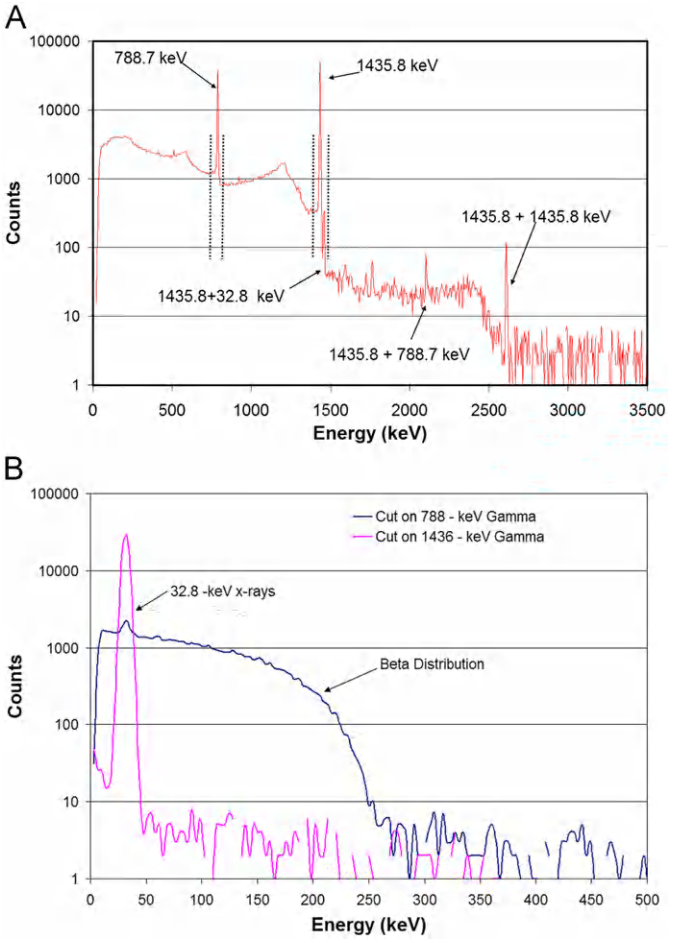


**Fig. 4.** (A) $LaCl_3$:Ce gated HPGe spectrum showing the dominant gamma-ray and gamma-ray sum peaks. (B) $LaCl_3$:Ce spectrum gated on the 788 and 1435 keV lines from the HPGe detector.

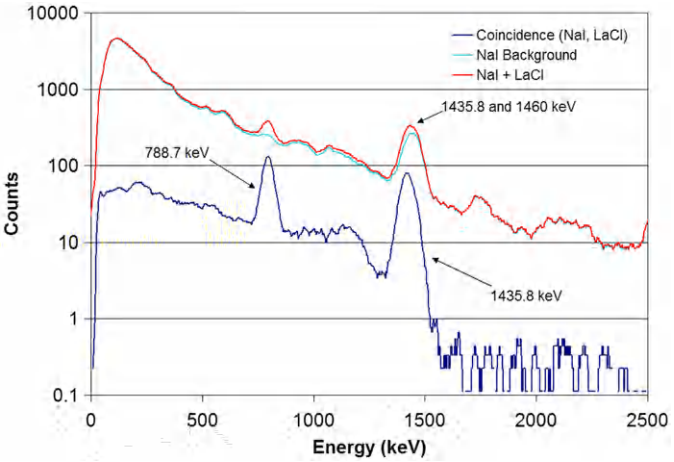


**Fig. 5.** NaI:Tl histograms. lower histogram is the coincidence spectrum while the two upper curves are the NaI:Tl measured with background (slightly lower of the upper curves) and the background with the LaCl3:Ce acting only as a source (no gating).

purposes and the detector must maintain its energy calibration once fielded. As with the NaI:Tl, the ability to use the gated gamma rays from a $LaCl_3$:Ce as both a detector efficiency calibration and an energy calibration source is possible.

## 4. Conclusions

The use of scintillators with entrained radioactivity can provide a very useful tool for field calibration of detectors. A complete understanding of the physics processes and the dominant signatures is important if a scintillator were to be made with radioactive isotopes. The new scintillator LaCl3:Ce with entrained $^{138}$La has several excellent properties for field calibration. It has two separate decay processes, which yield good gamma rays and excellent resolution to separate out backgrounds, and it has the reliability and robustness of a scintillator.

## Acknowledgement

This work was performed at the Pacific Northwest National Laboratory with Government support under Contract number DE-AC06-76RLO-1830 awarded by the United States Department of Energy, the Office of Nonproliferation Research and Engineering, and the Office of Research and Development.

## References

[1] O. Guillot-Noël, et al., J. Lumin. 85 (1999) 21.
[2] E.V.D. van Loef, et al., IEEE Trans. Nucl. Sci. NS-48 (3) (2001) 341.
[3] K. Alzimami, E. Abuelhia, Z. Podolyak, A. Ioannou, N.M. Spyrou, J. Radioanal. Nucl. Chem. 278 (3) .
[4] Saint-Gobain Crystals and Detectors, 104, Route de Larchant, 77140 Nemours, France, < http://www.detectors.saint-gobain.com/ > .
[5] W.J. Kernan, IEEE Nucl. Sci. Symp. Conf. Rec. 2 (2004) 1002.
[6] B.D. Milbrath, R. McIntyre, R.C. Runkle, T.W. Hossbach, W.R. Kaye, E.A. Lepel, B.S. McDonald, L.E. Smith, Nucl. Instr. and Meth. 547 (2005) 504;
B.D. Milbrath, R.C. Runkle, J.I. McIntyre, L.E. Smith, IEEE, Trans. Nucl. Sc. NS-53 (5) (2006) 3031, pt 2.
[7] R.B. Firestone, S.Y.F. Chu, C.M. Baglin, Table of Isotopes, eighth ed., Wiley, New York, 1999 CD_ROM.
[8] Edgardo Browne, R.B Firestone, WWW Table of Radioactive Isotopes, Version 2.1, < http://i.e.lbl.gov/toi/index.asp > (January 2004).
[9] Edgardo Browne, R.B. Firestone, Table of Radioactive Isotopes, eighth ed., Wiley, New York, 1996.
[10] Harshaw Polyscin, now affiliated with Bicron/Saint Gobain.
[11] W.K. Hensley, A.D. McKinnon, H.S. Miley, M.E. Panisko, R.M. Savard, J. Radioanal. Nucl. Chem. 193 (2) (1995) 229.
[12] ORTEC, 801S. Illinois Ave., Oak Ridge, TN 37831, USA, March 1997.
[13] W.K. Warburton, M. Momayezi, B. Hubbard-Nelson, W. Skulski, Appl. Radiat. Isot. 53 (4–5) (2000) 913.
[14] P.L. Reeder, T.W. Bowyer, J.I. McIntyre, W.K. Pitts, A. Ringbom, C. Johansson, Nucl. Instr. Meas. A 521 (2-3) (2004) 586.
[15] C. Hoel, L.G. Sobotka, K.S. Shah, J. Glodo, Nucl. Instr. and Meth. A 540 (2005) 205.